Mech Time-Depend Mater
https://doi.org/10.1007/s11043-019-09413-4

Tensile behaviors of thermal aged HTPB propellant at low temperatures under dynamic loading

Zhejun Wang[1] · **Hongfu Qiang**[1] · **Tiejun Wang**[2] ·
Guang Wang[1]

Received: 24 April 2018 / Accepted: 11 February 2019
© Springer Nature B.V. 2019

Abstract With the purpose of further investigating the influence of aging on the tensile behaviors of hydroxyl-terminated polybutadiene (HTPB) propellant at low temperatures under dynamic loading, uniaxial tensile stress responses of thermal accelerated aged propellant samples at different temperatures (223–298 K) and strain rates (0.40–42.86 s^{-1}) were obtained through the use of a new INSTRON testing machine. And scanning electron microscope (SEM) was employed to analyze the microscopic damage of HTPB propellant under the test conditions. Test results indicate that aging can significantly affect the characteristics of the stress-strain curves, mechanical properties and fracture mechanisms of HTPB propellant at low temperatures under dynamic loading. There are three regions in the tensile stress-strain curves of aged propellant when deforming at lower temperatures and the highest strain rate, however, there are five ones for unaged propellant. At lower temperatures and higher strain rates, the strain at maximum tensile stress of the propellant decreases more obviously after aging. Moreover, the variation of mechanical parameters for HTPB propellant with aging time are highly complex due to the occurrence of oxidative cross-linking during aging and the distinct changes of the fracture mechanisms. These variation were reasonably well described with linear model and the improved exponential model in this investigation. The fracture mechanism of aged propellant can change from dewetting, matrix tearing and AP particle fracture to only AP particle fracture with increasing strain rate for the entire test temperature range, and the strain rate for this transition is all at 4.00–14.29 s^{-1}. In addition, the microscopic damage of HTPB propellant becomes more severe with the thermal aging time rising, however, this effect is weaker at higher strain rates after long-time thermal aging. Finally, the master curves of typical mechanical parameters for aged HTPB propellant were constructed according to the time-temperature superposition principle (TTSP).

Keywords Tensile behavior · Accelerated aging · HTPB propellant · Low temperature · Dynamic loading

---

✉ Z. Wang
qinglongzaitian888@163.com

[1] 206 Staff room, Xi'an Hi-Tech Institute, Xi'an 710025, P.R. China

[2] MOE Key Laboratory for Strength and Vibration, Department of Engineering Mechanics, Xi'an Jiaotong University, Xi'an 710049, P.R. China

Published online: 19 February 2019

1 Introduction

Solid rocket motors (SRMs) are generally stored for different times before their actual flight, thus all SRMs are assigned a storage life up to which their safe operation can still be guaranteed (Yıldırım and Özüpek 2011). In most cases, the ultimate storage life of SRMs is determined by the structural integrity of solid propellant grains (Reeling Brouwer et al. 2005; Kadiresh and Sridhar 2010). This is because solid propellant is composed of large percentage of energetic components and classified as being in the family of high particle-filled elastomers. Its mechanical properties and microscopic damage may change due to a combination of chemical reactions and physical processes during prolonged storage, which normally results in a loss of the grain structural integrity (Bunyan et al. 1993; Reeling Brouwer and Keizers 2004). Therefore, it is necessary and very important to study the mechanical behaviors of solid propellant preserved over a long period of time to analyze and ensure the structural integrity of the solid propellant grain after long periods of storage.

Numerous attempts have been made in the past to understand the effect of aging on the properties of solid propellants (Kivity et al. 2005; Zhao et al. 2007; Goncalves et al. 2008; Trache and Khimeche 2013). In general, studying the change in properties of a propellant subjected to natural aging may take several years to obtain any result and it is time consuming. For this reason, the most common method is accelerated aging of a propellant at elevated temperatures higher than ambient temperature, then the change in properties during the aging period were determined in a reasonable time. Finally, the fastest reaction rate parameters will be selected for analysis. According to the thermal accelerated aging method, dynamic mechanical analysis (DMA) was widely employed to determine the changes in the dynamic mechanical properties of aged solid propellants, including the storage modulus and loss factor or damping efficiency, with accelerated aging time and aging temperature (Husband 1992; Cerri et al. 2013; de la Fuente and Rodrı´guez 2015). Moreover, differential scanning calorimetry (DSC) was usually applied for investigating the variation of the glass transition for solid propellants with the thermal accelerated ageing (Judge 2003; Rocco et al. 2004; de la Fuente 2009). From these test results, the aging rate of a propellant and the likely mechanisms occurring during aging were discussed. For example, composite solid propellants may degrade by oxidation of the polybutadiene matrix and loss of plasticizer by migration and evaporation, etc. (Rocco et al. 2004; de la Fuente 2009). Though these two test methods can use a very small amount of sample to provide the aging characterization and service life assessment with a quick and easy procedure, and the test results are helpful to understand the properties of solid propellants in depth, the failure properties and stress-strain data of aged solid propellants cannot be attained with them, meaning that it is difficult to analyze the structural integrity of the solid propellant grain. Conversely, through a uniaxial testing machine, lots of mechanical experiments had been conducted on the accelerated aged solid propellant samples under quasi-static (usually from 0.0001 to 1 s^{-1}) loading (Hocaoğlu et al. 2001; Kadiresh and Sridhar 2008; Shekhar 2012). Subsequently, the effect of aging on the mechanical properties (for example, elasticity modulus, maximum tensile stress or tensile strength and the corresponding elongation, etc.) for a propellant were investigated. Test results obtained reveal that elasticity modulus and tensile strength of aged solid propellants usually increase overall, whereas the corresponding elongation has a significant decline. To describe the relationships of these typical mechanical parameters for solid propellants with accelerated aging time, linear, exponential or logarithmic aging model has been widely used in the past decades (Layton 1975; Andersen and Bruno 2005). In addition, external factors (for example, pre-strain conditions and accelerated aging temperature, etc.) can further affect the above mechanical properties of aged solid propellants (Kishore et al. 1979; Jalocha et al. 2015), and those empirical aging models had been modified recently by defining the model parameter as a function of external factors (Cerri et al. 2009; Zhou et al. 2016). Based on the obtained properties of aged solid propellants under quasi-static loading, some failure criteria had been developed and the structural integrity of the solid propellant grain after long periods of storage was analyzed (Villar et al. 2011; Deng et al. 2015).

During ignition of SRM for the tactical missiles at low temperatures, the propellant has to withstand the coupled effects of low temperature and dynamic loading (1–100 s^{-1}) (Jeremic 1999; Jiang et al. 2011; Chu and Chou 2013). In our previous work (Wang et al. 2015a, 2015b, 2016a, 2016b, 2018), the tensile and compressive behaviors of a propellant over the range of temperatures 223 to 298 K and strain rates 0.40 to 63 s^{-1} were successfully studied for the first time using a new INSTRON testing machine. Besides, the variation of the glass transition temperature for the propellant with different loading conditions had also been discussed. Test results reveal that the mechanical properties and fracture mechanisms of solid propellant at low temperatures under dynamic loading (1–100 s^{-1}) are highly complex and different from that obtained at other loading conditions. Thereby, to ensure the structural integrity of the solid propellant grain for the tactical missiles during ignition at low temperatures after long periods of storage, it is extremely necessary to investigate the behaviors of aged solid propellant at low temperatures under dynamic loading (1–100 s^{-1}). However, the related research is very limited in the current literature, which provokes the requirement of the new test methods and analysis theories.

In the presented paper, thermal accelerated aging programs on hydroxyl-terminated polybutadiene (HTPB) propellant blocks were carried out firstly. Then uniaxial tensile tests were performed on the propellant samples to investigate the mechanical properties of aged propellant at low temperatures under dynamic loading (1–100 s^{-1}). Meanwhile, a scanning electron microscope (SEM) was employed to observe the fracture surfaces. Afterward, the coupled effects of the temperature, strain rate and aging on the tensile behaviors of HTPB propellant were discussed based on the test results. Finally, with the aim of predicting the mechanical properties under different loading conditions, the master curves of typical mechanical parameters for aged HTPB propellant were constructed according to the time-temperature superposition principle (TTSP). Besides, the suitable models were selected or proposed to describe the relationships of the mechanical parameters with aging time.

2 Experiments

2.1 Materials and sample preparation

The HTPB-based composite solid propellant was selected for this study, and it has the following compositions: 60.0 mass-% of larger ammonium perchlorate (AP), 9.5 mass-% of smaller AP, 18.5 mass-% of Aluminium (Al) powder, 6.0–7.0 mass-% of HTPB, 3.4 mass-% of dicapryl sebacate (DOS), 1.0–2.0 mass-% of toluene diisocyanate (TDI), 0.05–0.1 mass-% of tris 1(2 methylazirindinyl) phosphine oxide (MAPO) and 0.5–1.0 mass-% of other liquid additives.

All formulations were prepared in a vertical kneader and cured in an oven cabinet for 7 days at 323.15 K. According to the Chinese aerospace industry standard of P. R. C, QJ 2328A-2005, the samples of freshly mixed and cured propellant were cut into blocks with dimensions of 120 mm × 130 mm × 30 mm.

Fig. 1 The new uniaxial testing machine INSTRON VHS 160/100-20

2.2 Accelerated ageing experiments

The thermal accelerated aging experiments were carried out in temperature-controlled (±1 K, stability) commercial air circulating aging ovens. The propellant blocks were subjected to accelerated aging for over 98 days at the temperature of 343.15 K, with RH $< 10\%$ and in load-free condition (no pre-strain). At the scheduled intervals of time during the aging period, the propellant blocks were removed to measure the mechanical properties of the propellant.

2.3 Tensile tests

To avoid the effects of moisture and viscoelastic recovery on the tensile behaviors of the propellant, the aged propellant blocks were firstly put into a dryer until they no longer shrunk, and the geometrical dimensions were constant. Then these blocks were further cut into individual dumbbell-slat samples for uniaxial tensile tests according to the Chinese aerospace industry standard of P.R. C, QJ 924-85, and the dimensions of the samples are consistent with that in our previous work (Wang et al. 2015b). Uniaxial tensile tests were still performed through using the new designed gripping jaws and testing machine INSTRON VHS 160/100-20 (as shown in Fig. 1), which can apply the displacement through the shoulders of the sample and guarantee the dynamic loading (1–100 s^{-1}) conditions required in this investigation. Testing was conducted at five temperatures (223, 233, 243, 253, and 298 K) and four constant crosshead rates (28, 280, 1000, and 3000 mm/s, namely, 0.40, 4.00, 14.29, and 42.86 s^{-1}). The sample test matrix is shown in Table 1. Prior to testing, the samples were sealed with plastic film and preconditioned at the test temperature for 1 h. Besides, the humidity of the temperature chamber was controlled below 5%. The samples were pulled to failure finally, and the INSTRON software recorded the load and displacement. More detailed information about the test setup and the tensile processing with the testing machine INSTRON VHS 160/100-20 had been stated in our previous work (Wang et al. 2015b, 2016b), please refer to them. In this paper, the tensile test was repeated for five times at each loading condition (temperature, strain rate and aging time). The stress σ, strain ε and strain rate $\dot{\varepsilon}$ were calculated from Eqs. (1a)–(1c) with the recorded data, and then the

Table 1 Sample test matrix

Thermal accelerated aging time [d]	Temperature [K]	Strain rate [s^{-1}]			
32	298	0.40	4.00	14.29	42.86
	253	0.40	4.00	14.29	42.86
	243	0.40	4.00	14.29	42.86
	233	0.40	4.00	14.29	42.86
	223	0.40	4.00	14.29	42.86
74	298	0.40	4.00	14.29	42.86
	253	0.40	4.00	14.29	42.86
	243	0.40	4.00	14.29	42.86
	233	0.40	4.00	14.29	42.86
	223	0.40	4.00	14.29	42.86
98	298	0.40	4.00	14.29	42.86
	253	0.40	4.00	14.29	42.86
	243	0.40	4.00	14.29	42.86
	233	0.40	4.00	14.29	42.86
	223	0.40	4.00	14.29	42.86

corresponding curves were plotted. All stress-strain curves investigated in the following sections were the average of these five curves after excluding the outlier ones according to the Chinese national standard of P. R. C, GJB 770B-2005.

$$\sigma = F/A \tag{1a}$$

$$\varepsilon = (L - L_0)/L_0 = \Delta H/L_0 \tag{1b}$$

$$\dot{\varepsilon} = \varepsilon/t = V/L_0 \tag{1c}$$

where F is the tensile load; A, L_0 and L represents the original cross-sectional area (10 mm × 10 mm), original length (70 mm) and current length of the test sample, respectively; t and ΔH are the loading time and displacement of the top platen from the start of the tensile test; V is the loading speed of the testing machine in tension.

After the tensile tests, pieces of propellant (10 × 10 × 5 mm) were cut out from the fracture location of the test samples for routine post-failure examination. And SEM analyses were performed on a Quanta 600FEG SEM.

3 Results and discussion

3.1 Analysis of constant strain rate

The constant of the engineering strain rate $\dot{\varepsilon}$ during dynamic loading must be verified to ensure that the obtained characteristics of the sample were intrinsic properties of the test material. Figure 2 presents the relationships between stress and time, strain rate and time under the typical test conditions. It can be seen from Fig. 2 that the strain rate is constant during loading as a whole expect the small oscillation at the initial loading process (before point A). Because this small oscillation occurs at the short time less than 10% of the total

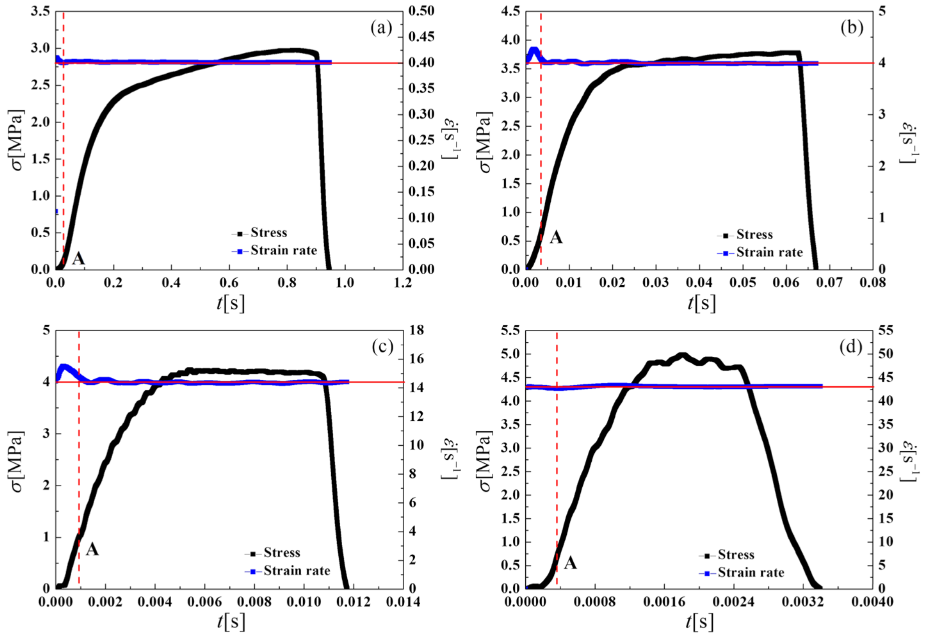

Fig. 2 Typical loading cases of the samples under the test conditions. (**a**) 233 K, 0.40 s^{-1} and 98 d; (**b**) 233 K, 4.00 s^{-1} and 98 d; (**c**) 233 K, 14.29 s^{-1} and 98 d; (**d**) 233 K, 42.86 s^{-1} and 98 d. "A" is the starting point beyond which the engineering strain rate is constant

loading time, the requirement of constant engineering strain rate can be satisfied, and the test data obtained are valid in this investigation.

3.2 Stress-strain curves and mechanical properties

The typical tensile stress-strain curves of HTPB propellant under the test conditions are shown in Fig. 3. It can be seen from Fig. 3 that the characteristics of stress-strain curves are quite similar for aged and unaged propellant (refer to our previous work, Wang et al. 2015b). The propellant still displays nonlinear material behaviors in dynamic tension after aging. Meanwhile, temperature and strain rate still remarkably influence the tensile behaviors of aged HTPB propellant. The stress continuously increases as strain rate increases or temperature decreases. However, the most remarkable difference is that there are three regions in the tensile stress-strain curves of aged propellant when deforming at lower temperatures (233–253 K) and the highest strain rate, in other words, a strain softening region disappears before the maximum stress, as shown in Figs. 3(b)–(c) and 4. Instead, there are five ones for unaged propellant, as found in our previous work (Wang et al. 2015b, 2016b).

Based on the above test results, the elasticity modulus E (through the point A in the conventional manner), maximum tensile stress σ_m and the corresponding strain ε_m were directly defined on the stress–strain curves with the method as shown in Fig. 4. Then the variation of these typical mechanical parameters for HTPB propellant with strain rate at various tensile test temperatures are shown in Fig. 5. It can be concluded from Figs. 5(a)–(b) that the effects of temperature and strain rate on the elasticity modulus E and maximum tensile stress σ_m for

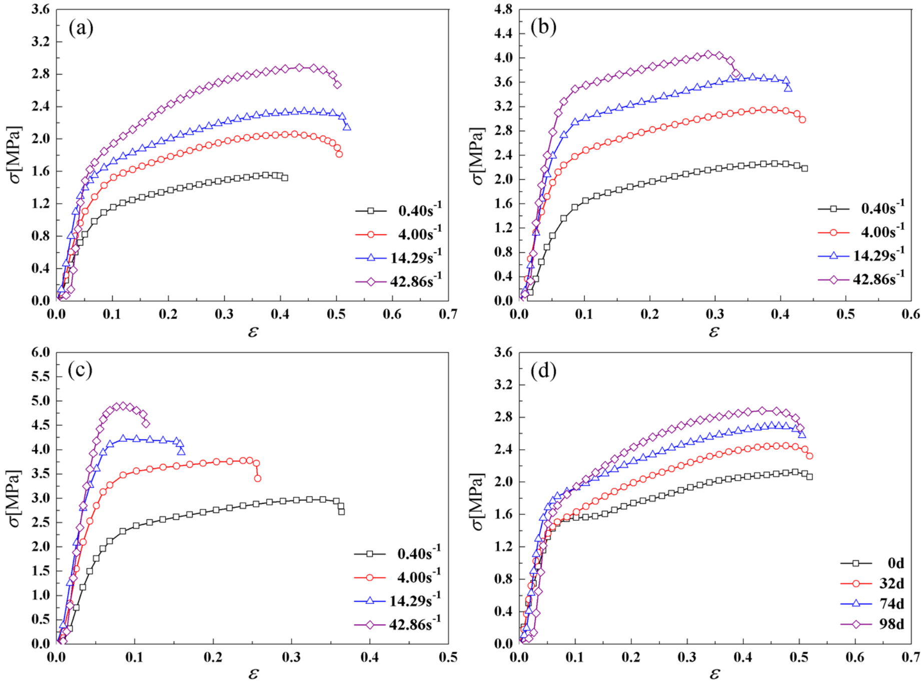

Fig. 3 Typical stress-strain curves of the tensile tests for HTPB propellant under the test conditions. (**a**) 298 K and 98 d; (**b**) 253 K and 98 d; (**c**) 233 K and 98 d; (**d**) 298 K and 42.86 s^{-1}

Fig. 4 Schematic diagram of uniaxial tensile stress–strain curves for aged and unaged HTPB propellant at lower temperatures and the highest strain rate

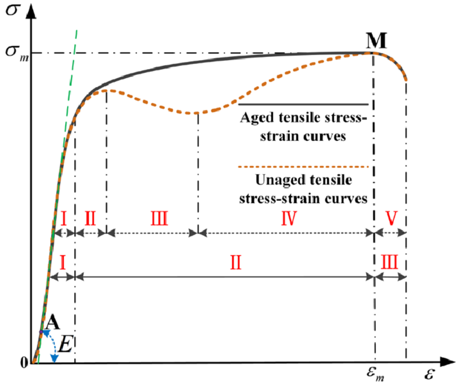
σ
σm
M
Aged tensile stress-strain curves
Unaged tensile stress-strain curves
I
II
III
IV
V
I
II
III
A
E
0
εm
ε

aged propellant are the same as that without aging (refer to our previous work, Wang et al. 2015b). These two mechanical parameters all still increase gradually with increasing strain rate, and present linear-log relationships with strain rate. However, the effects of temperature and strain rate on the strain at maximum tensile stress ε_m of the propellant are complex, as shown in Figs. 5(c)–(d). Before and after aging, the maximal value of the strain ε_m all can be obtained at room temperature and the strain rate of 14.29 s^{-1}, then it decreases with continuously increasing strain rate. At low temperatures, this strain decreases as a whole when strain rate becomes higher. Whereas, it is constant at the lowest temperature and higher strain rates. The most remarkable difference for aged and unaged propellant is that the strain

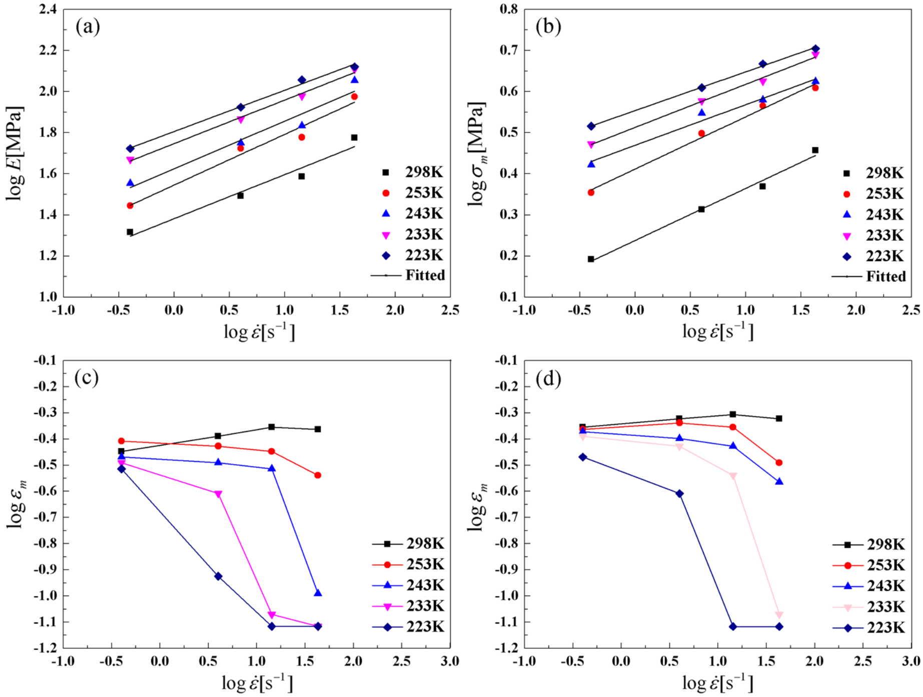

Fig. 5 The variation of the typical mechanical parameters for HTPB propellant with strain rate at various tensile test temperatures. (**a**) Elasticity modulus after aging for 98 d; (**b**) maximum tensile stress after aging for 98 d; (**c**) strain at maximum tensile stress after aging for 98 d; (**d**) strain at maximum tensile stress without aging

ε_m decreases more obviously at the lower temperatures and higher strain rates after aging. In addition, at the lowest strain rate of 0.40 s^{-1}, the maximal value of the strain ε_m obtained at 253 K after aging (as shown in Fig. 5(c)). However, Fig. 5(d) shows that the strain ε_m decreases with the temperature continuously decreasing for unaged propellant.

The variation of the typical mechanical parameters for HTPB propellant with aging time under the tensile test conditions are shown in Fig. 6. As seen, thermal accelerated aging has a pronounced effect on the mechanical properties of HTPB propellant. An increment in the elasticity modulus E (Figs. 6(a)–(c)) and in the maximum tensile stress σ_m (Figs. 6(d)–(f)), as well as a decreasing in the strain ε_m (Figs. 6(g)–(i)) are found. Moreover, the variation trend of these mechanical parameters are complex and different from each other. The elasticity modulus E varies linearly with aging time under all tensile test conditions (Figs. 6(a)–(c)), which is consistent with most previous results at room temperature and quasi-static loading (Kadiresh and Sridhar 2008). Meanwhile, the aging load causes a more significant increase of the modulus E at the highest strain rate. Figures 6(d)–(f) show that the relationships of the maximum tensile stress σ_m with aging time under the test conditions are nonlinear, which is different from that found at room temperature and quasi-static loading (Kadiresh and Sridhar 2008). In addition, the tensile stress σ_m seems to be more affected by aging time at higher strain rates. Especially, a great increment in this mechanical parameter is found at further stages of aging when testing at 233 K and the highest strain rate, as shown in Fig. 6(f). From Figs. 6(g)–(i), a linear dependence of the strain ε_m with aging time was observed at room temperature or at low temperatures and the strain rates of 0.40 and

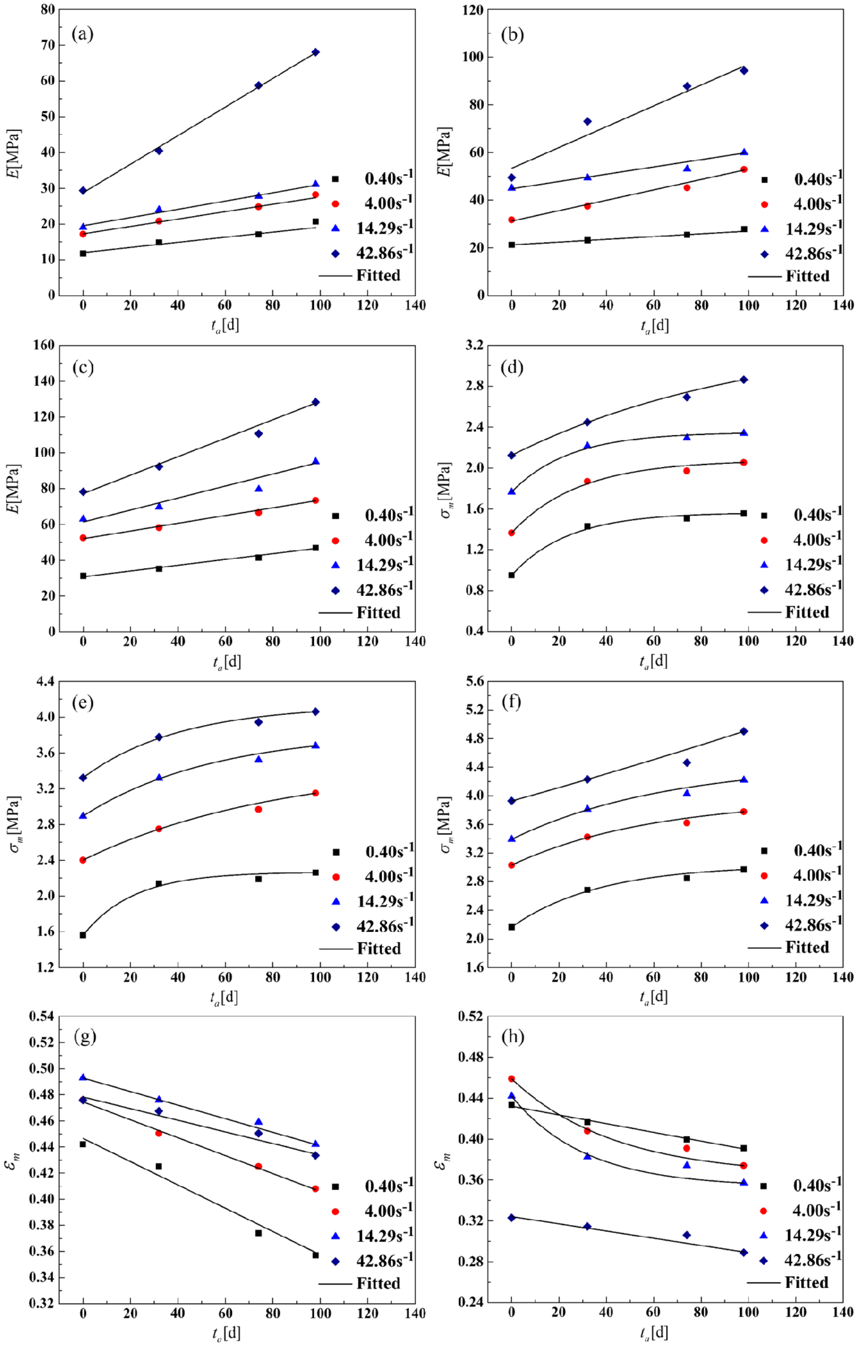

Fig. 6 The variation of the typical mechanical parameters for HTPB propellant with aging time under the tensile test conditions. (**a**) Elasticity modulus at 298 K; (**b**) elasticity modulus at 253 K; (**c**) elasticity modulus at 233 K; (**d**) maximum tensile stress at 298 K; (**e**) maximum tensile stress at 253 K; (**f**) maximum tensile stress at 233 K; (**g**) strain at maximum tensile stress at 298 K; (**h**) strain at maximum tensile stress at 253 K; (**i**) strain at maximum tensile stress at 233 K

Fig. 6 (*Continued*)

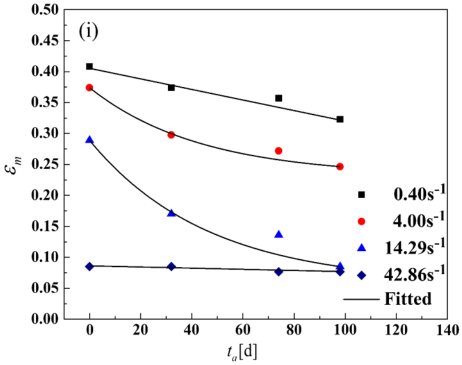

42.86 s^{-1} (the lowest and highest strain rate). This trend is in agreement with some results stated previously at room temperature and quasi-static loading (Kadiresh and Sridhar 2008). Nevertheless, the nonlinear variation is found between the strain ε_m and aging time at low temperatures and higher strain rates, from 4.00 to 14.29 s^{-1}.

3.3 Fracture mechanism

According to the previous research (Bohn and Volk 1992; Celina et al. 2002), oxidative cross-linking may be the dominant chemical mechanism during accelerated ageing in this investigation, which can cause the rising trend of the elasticity modulus E and the maximum tensile stress σ_m, whereas the decline of the strain at maximum tensile stress ε_m. However, the changes of the stress σ_m and strain ε_m for aged HTPB propellant are dependent on not only the chemical mechanisms during accelerated aging, but also the occurrence and propagation of microcracks in itself under various loading conditions. The typical SEM images of the tensile fracture surfaces for different aged HTPB propellant at various temperatures and strain rates are shown in Fig. 7.

Solid propellant is highly particle-filled elastomer, namely, it is made by embedding some divided solid particles (such as AP, Al) in an elastomeric matrix. Therefore, the fracture mechanisms (or microscopic damage) of the propellant usually include the filler/matrix interface fail (namely, dewetting), matrix tearing and solid particles fracture. During thermal accelerated ageing, the matrix hardens and the interface adhesive stress between AP particles and the matrix decreases due to the thermal stress. Then adhesive interface fail (or dewetting) for the propellant is much more likely to occur as aging time increases. In addition, thermal stress loading can induce the slow decomposition of AP particles, and this ultimately results in AP particles fracture. Hence, a dewetting phenomenon (pulling out of binder from filler particles) and AP particles fracture all can be observed at the lowest strain rate, as shown in Figs. 7(a)–(b) and Figs. 7(e)–(f). However, the dominating fracture mechanism of unaged HTPB propellant is only the dewetting at room temperature and the lowest strain rate (Fig. 7(a) in our previous work, Wang et al. 2015b), and is only some AP particles fracture at low temperature and the lowest strain rate (Fig. 7(d) in our previous work, Wang et al. 2015b). Because the damage of HTPB propellant is more complex and severe with increasing aging time at the lowest strain rate, the strain at maximum tensile stress ε_m continues decreasing linearly, as shown in Figs. 7(g)–(i). Furthermore, the propellant becomes stiffer on decreasing the temperature, consequently, the interface adhesive stress is higher at low temperature. From the above discussions, the damage of aged HTPB propellant is slighter at 253 K and the lowest strain rate than that at room temperature and the lowest

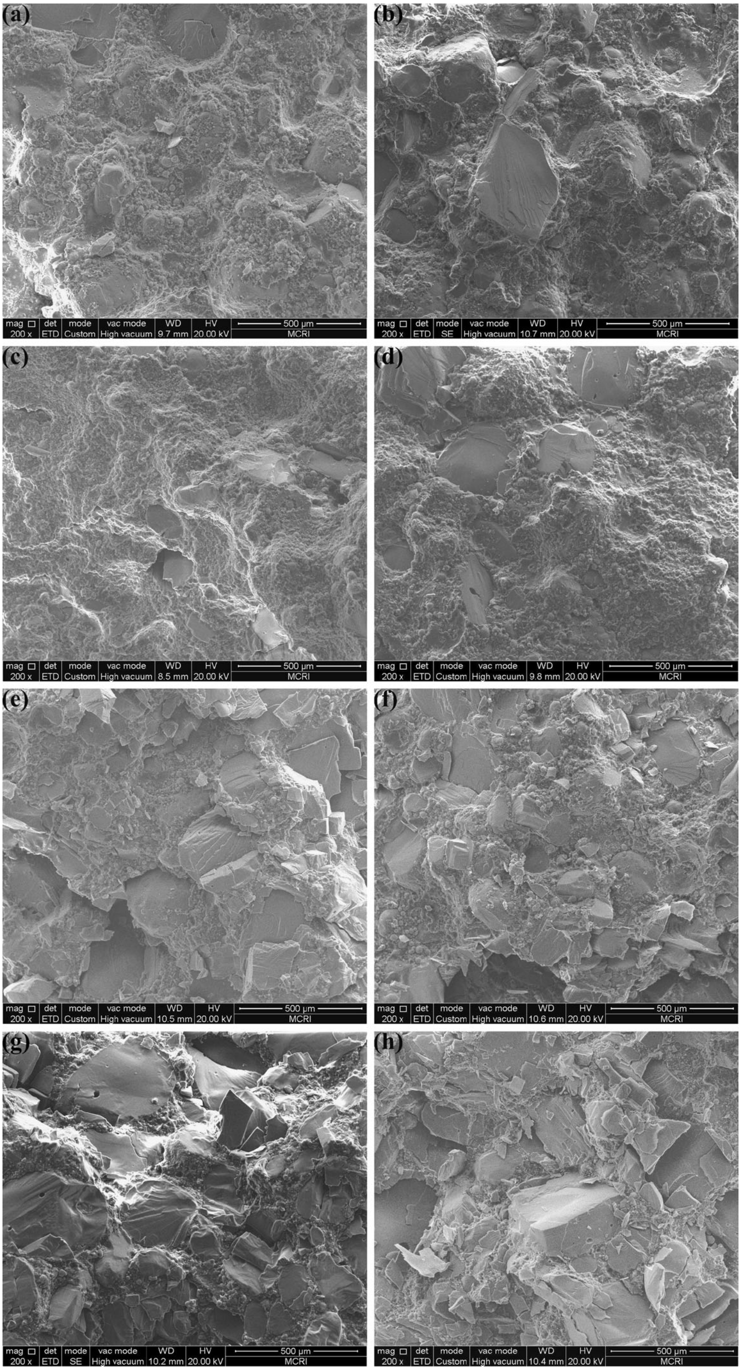
(a)
mag □ | det | mode | vac mode | WD | HV | 500 μm
200 x | ETD | Custom | High vacuum | 9.7 mm | 20.00 kV | MCRI
(b)
mag □ | det | mode | vac mode | WD | HV | 500 μm
200 x | ETD | SE | High vacuum | 10.7 mm | 20.00 kV | MCRI
(c)
mag □ | det | mode | vac mode | WD | HV | 500 μm
200 x | ETD | Custom | High vacuum | 8.5 mm | 20.00 kV | MCRI
(d)
mag □ | det | mode | vac mode | WD | HV | 500 μm
200 x | ETD | Custom | High vacuum | 9.8 mm | 20.00 kV | MCRI
(e)
mag □ | det | mode | vac mode | WD | HV | 500 μm
200 x | ETD | Custom | High vacuum | 10.5 mm | 20.00 kV | MCRI
(f)
mag □ | det | mode | vac mode | WD | HV | 500 μm
200 x | ETD | Custom | High vacuum | 10.6 mm | 20.00 kV | MCRI
(g)
mag □ | det | mode | vac mode | WD | HV | 500 μm
200 x | ETD | SE | High vacuum | 10.2 mm | 20.00 kV | MCRI
(h)
mag □ | det | mode | vac mode | WD | HV | 500 μm
200 x | ETD | Custom | High vacuum | 10.4 mm | 20.00 kV | MCRI

Fig. 7 The typical SEM images of the tensile fracture surfaces for different aged HTPB propellant at various temperatures and strain rates. (**a**) 298 K, 0.40 s^{-1} and 74 d; (**b**) 298 K, 0.40 s^{-1} and 98 d; (**c**) 298 K, 14.29 s^{-1} and 74 d; (**d**) 298 K, 14.29 s^{-1} and 98 d; (**e**) 233 K, 0.40 s^{-1} and 74 d; (**f**) 233 K, 0.40 s^{-1} and 98 d; (**g**) 233 K, 14.29 s^{-1} and 74 d; (**h**) 233 K, 14.29 s^{-1} and 98 d

strain rate, which further leads to the higher value of the strain ε_m at 253 K after aging (as shown in Fig. 5(c)).

As strain rate is up to 14.29 s^{-1}, there is not enough time for microcracks to propagate to the interface between the matrix and solid particles, consequently, the particles are still coated with matrix and the dewetting for solid propellant is much slighter, as shown in Figs. 7(c)–(d) and Figs. 7(g)–(h). Because of these, the strain ε_m of aged HTPB propellant still increases with increasing strain rate at room temperature. However, continuously increasing the strain rate can result in higher tensile stress, thus, more AP particle fractures occur. Namely, the damage of aged HTPB propellant is more severe again at room temperature and the strain rate of 42.86 s^{-1}, thus, the strain ε_m decreases again, as shown in Fig. 5(c). At low temperatures, it is easier for microcracks to initiate and grow in the AP particles since the interface adhesive stress is higher. Consequently, more AP particles fractures occur as strain rate continues increasing at low temperatures because of the higher stress wave accompanying with tensile loading. Based on these, the strain ε_m of aged HTPB propellant decreases constantly with increasing strain rate at low temperatures, as shown in Fig. 5(c). Furthermore, as discussed above, thermal stress loading can induce AP particles fracture. Therefore, on the one hand, the strain ε_m of HTPB propellant also decreases with aging time at strain rates higher than 0.40 s^{-1}. On the other hand, the strain ε_m of aged HTPB propellant decreases more obviously at the lower temperatures and higher strain rates than that without aging (companying Figs. 5(c) and (d)). With the coupled effects of long-term aging, lower temperature and higher strain rate, lots of AP particles are disrupted, which means that the damage of HTPB propellant is very severe and is nearly independent on the external factors (Figs. 7(g)–(h)). Then the strain ε_m of HTPB propellant is almost constant with the variation of strain rate and aging time at the temperatures of 223–233 K, as shown in Fig. 5(c) and Fig. 6(i).

For unaged HTPB propellant, there is a strain softening region before the maximum tensile stress at the lower temperatures of 243–253 K and the highest strain rate of 42.86 s^{-1} (Wang et al. 2015b). As analyzed in our previous work (Wang et al. 2015b), this results from a large amount of AP particles fracture at small strain under those test conditions. Meanwhile, the propellant is still in viscoelastic state and is still capable of large deformation under those test conditions. Thereby, the stress increases again beyond that softening region in the stress-strain curve due to the strain hardening of the matrix. In this investigation, more AP particles fracture occur at small strain after aging. In addition, the glass transition temperature of the propellant may be higher due to thermal aging and the propellant hardens, which means that the molecular mobility of the matrix chains is obviously reduced and the strain hardening of the matrix is not obvious. Therefore, for aged HTPB propellant, the strain softening region before the maximum tensile stress in the stress-strain curve does not present clearly.

As stated in our previous work (Wang et al. 2015b), strain rate only can alter the dominating fracture mechanism of unaged HTPB propellant at room temperature, and the value for the transition from dewetting and matrix tearing to AP particle fracture is at 14.29–42.86 s^{-1}. Meanwhile, the damage of unaged HTPB propellant at low temperature is only affected in a quantitative manner with continuously increasing strain rate. However, the above results and discussions suggest that temperature, strain rate and aging can change the dominating fracture mechanism of HTPB propellant in this investigation. The strain rate for the transition from dewetting, matrix tearing and AP particle fracture to only AP particle fracture is at 4.00–14.29 s^{-1} for the entire test temperature range. Because of this transition at 4.00–14.29 s^{-1}, the variation of the strain ε_m with aging time is nonlinear.

In this investigation, the strain at maximum tensile stress ε_m decreases overall with the coupled effects of the lower temperature, higher strain rate and long-term aging. The value

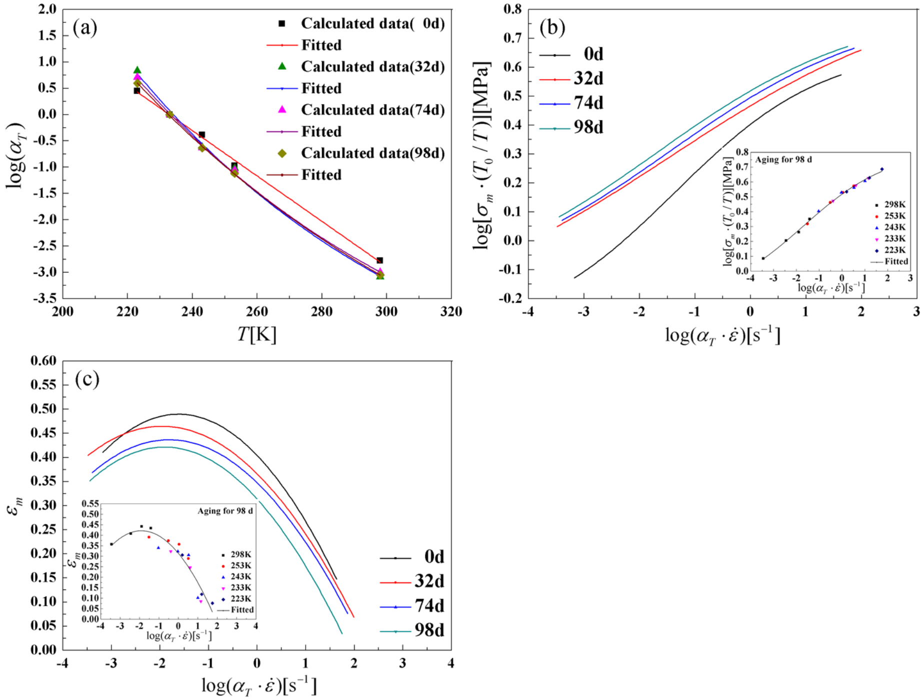

Fig. 8 The typical master curves of the mechanical parameters for HTPB propellant reduced to 233 K. (**a**) Logarithmic shift factor; (**b**) maximum tensile stress; (**c**) strain at maximum tensile stress

of the strain ε_m at 223 K and 42.86 s^{-1} after aging for 98 d reduces to 15.52% of its maximum value without aging. In addition, this strain can reflect the changes of the fracture mechanisms for HTPB propellant. Therefore, based on the general principles of the analysis (Gligorijević et al. 2015), this parameter can be selected as a fail criterion for analyzing the structural integrity of the solid propellant grain for the tactical missiles during ignition at low temperatures after long periods of storage.

3.4 Master curve and aging model

The master curve is usually applied for predicting the mechanical properties of highly particle-filled elastomers in wide intervals of temperatures and strain rates. According to TTSP, the master curves of the mechanical parameters for aged HTPB propellant were constructed with the reference temperature of 233 K. The typical ones are shown in Fig. 8. As can be seen clearly, the trend of the logarithmic shift factor $\log(\alpha_T)$ is nonlinear with temperature after aging, which is not consistent with that obtained for unaged HTPB propellant (Fig. 8(a)). In addition, the relevant curves for aged propellant almost coincide with each other. However, all master curves of the propellant are nonlinear in form before and after aging (Figs. 8(b)–(c)). The relationships of the maximum tensile stress σ_m and the corresponding strain ε_m with the reduced strain rate $\log(\alpha_T \cdot \dot{\varepsilon})$ after aging can be described by the following expression, respectively:

$$\log\left[\sigma_m \cdot (T_0/T)\right] = A_1 + \frac{A_2}{1 + \exp[A_3 \log(\alpha_T \cdot \dot{\varepsilon}) + A_4]} \tag{2}$$

Table 2 Value of constants of the master curve for HTPB propellant

	Constant	Thermal aging time [d]		
		32	74	98
Maximum tensile stress σ_m	A_1 [MPa]	0.8883	0.8094	0.8128
	A_2 [MPa]	−1.2010	−2.6913	−1.0210
	A_3 [MPa]	0.4181	0.5383	0.5296
	A_4 [MPa]	0.6164	0.7787	0.9054
	Regression coefficient	0.9980	0.9983	0.9966
Strain at maximum tensile stress ε_m	B_1	−11.2768	−7.0573	−5.6820
	B_2	11.7415	7.4940	6.1035
	B_3	0.0332	0.0427	0.0495
	B_4	0.0650	0.0774	0.0944
	Regression coefficient	0.8726	0.8859	0.8754
Logarithmic shift factor $\log(\alpha_T)$	C_1 [s^{-1}]	71.7152	64.1747	49.6454
	C_2 [K^{-1}]	96.6340	100.6040	121.6268
	C_3 [s^{-1}]	−6.3569	−6.3183	−7.3343
	Regression coefficient	0.9944	0.9979	0.9996

$$\varepsilon_m = B_1 + B_2 \exp\left\{-2 \times \left[B_3 \log(\alpha_T \cdot \dot{\varepsilon}) + B_4\right]^2\right\} \tag{3}$$

$$\log(\alpha_T) = C_1 \exp(-T/C_2) + C_3 \tag{4}$$

where T_0 is the reference temperature and its value is defined as 233 K, A_1, A_2, A_3, A_4, B_1, B_2, B_3, B_4, C_1, C_2 and C_3 are "best-fit" constants. The related values of these constants for aged HTPB propellant can be seen Table 2.

Substituting Eq. (4) into Eqs. (2) and (3), the following expressions can be further developed:

$$\sigma_m = T/T_0 \times 10^{A_1 + \frac{A_2}{1+\exp[A_3 \log\dot{\varepsilon} + l_1 \exp(l_2 \cdot T) + l_3]}} \tag{5}$$

$$\varepsilon_m = B_1 + B_2 \exp\left\{-2 \times \left[B_3 \log\dot{\varepsilon} + l_4 \exp(l_2 \cdot T) + l_5\right]^2\right\} \tag{6}$$

where l_1 $(= A_3 \times C_1)$, l_2 $(= -1/C_2)$, l_3 $(= A_3 \times C_3 + A_4)$, l_4 $(= B_3 \times C_1)$ and l_5 $(= B_3 \times C_3 + B_4)$ are material constants.

The aging processes have been well described with the Layton equations, including linear, exponential and logarithmic models (Layton 1975):

$$P = P_0 + K t_a \tag{7a}$$

$$P = P_0 \exp(-K t_a) \tag{7b}$$

$$P = P_0 + K \log t_a \tag{7c}$$

where P is the property at any time of aging, P_0 is the property at referred time (unaged), K is the ageing rate constant (d^{-1}), t_a is the aging time (d).

Based on the analyses in the anterior section, Eq. (7a) was employed to describe the linear variations of the mechanical parameters with aging time in Fig. 6. However, the nonlinear variations in Fig. 6 cannot be described well by Layton equations. Thus, the following improved model was proposed in this investigation:

$$P = P_0 + \beta \exp(-K t_a) \tag{8}$$

where β is defined as the ageing constant.

The test data at 0, 32 and 98 d were applied for determining the model parameters in Eqs. (7a) and (8) with the Levenberg-Marquardt optimization method in this study, and the related values are shown in Table 3. In addition, other test data were used for the validation of the models. From Fig. 6, it can be seen that the overlap between experimental results and predicted results are generally good, which indicates that the selected or proposed model can offer a good description.

According to the previous research (Zou et al. 1996; Edidin et al. 2000; Cerri et al. 2009; Trache and Khimeche 2013), test results with accelerated aging and natural aging are complementary when predicting the service life of nonmetallic materials. Besides, test results with the former method can be employed to predict the properties of these materials after preserved over a long period of time at natural environment, when the aging mechanisms of the materials are consistent with each other under the two loading conditions. The variation tendency of the typical mechanical parameters for HTPB propellant with accelerated aging time in this investigation are the same as that obtained after natural aging in previous research (Lloyd 1977; Gligorijević et al. 2016). Therefore, the maximum tensile stress σ_m and the corresponding strain ε_m under different loading conditions (temperature, strain rate and aging time) can be predicted with the flow chart of solution as shown in Fig. 9, on the basis of Eqs. (5), (6), (7a) and (8). Moreover, these predicted results will be further validated by comparing them with the test data obtained at the same temperature and strain rate after preserved over a long period of time at natural environment in the future work.

4 Conclusions

The uniaxial tensile tests of aged HTPB-based solid propellant at low temperatures under dynamic loading (1–100 s^{-1}) were successfully performed for the first time by means of the thermal accelerated aging test method and the new INSTRON testing machine. According to the tensile test results and SEM analysis, the uniaxial tensile behaviors of aged HTPB propellant are still remarkably affected by temperature and strain rate. In addition, aging process causes significant changes in the characteristics of stress-strain curves, mechanical properties and fracture mechanisms for the propellant. The elasticity modulus E increases linearly with increasing aging time under all tensile test conditions. Continuously increasing the aging time causes a nonlinear increment of the maximum tensile stress σ_m under the test conditions. A linear decrease of the strain at maximum tensile stress ε_m with increasing aging time was found at room temperature or at low temperatures and the strain rates of 0.40 and 42.86 s^{-1}. Nevertheless, the value of this strain reduces nonlinearly as aging time increases at low temperatures and higher strain rates, from 4.00 to 14.29 s^{-1}. The changes in the characteristics of the stress-strain curves and mechanical properties for aged HTPB propellant are closely related to the oxidative cross-linking chemical mechanism and the more complex and severe fracture mechanisms. The strain rate for the transition from dewetting, matrix tearing and AP particle fracture to only AP particle fracture is at 4.00–14.29 s^{-1} at all test temperatures. The above test results are helpful for researchers to achieve a deeper

Table 3 Value of aging model parameters for HTPB propellant

Mechanical parameter	Temperature [K]	Strain rate [s^{-1}]	Model parameters		
			P_0	β	K
Elastic modulus E [MPa]	298	0.40	12.0258	–	0.07119
		4.00	17.2804	–	0.1030
		14.29	19.5062	–	0.1155
		42.86	28.7572	–	0.3993
	253	0.40	21.3011	–	0.05706
		4.00	31.2556	–	0.2180
		14.29	44.7815	–	0.1530
		42.86	53.3548	–	0.4372
	223	0.40	30.7699	–	0.1613
		4.00	52.0290	–	0.2160
		14.29	61.3851	–	0.3348
		42.86	77.2188	–	0.5160
Maximum tensile stress σ_m [MPa]	298	0.40	1.5651	−0.6156	0.04187
		4.00	2.0775	−0.7125	0.03512
		14.29	2.3507	−0.5864	0.04088
		42.86	3.3276	−1.2046	9.7468×10^{-3}
	253	0.40	2.2683	−0.7077	0.04691
		4.00	3.4789	−1.0783	0.01209
		14.29	3.8365	−0.9438	0.01821
		42.86	4.1343	−0.8123	0.02449
	223	0.40	3.0309	−0.8662	0.02712
		4.00	3.9516	−0.9206	0.01692
		14.29	4.4562	−1.0652	0.01537
		42.86	−2.1980	6.1258	-1.5052×10^{-3}
Strain at maximum tensile stress ε_m	298	0.40	0.4466	–	-8.9175×10^{-4}
		4.00	0.4746	–	-6.8640×10^{-4}
		14.29	0.4929	–	-5.1962×10^{-4}
		42.86	0.4783	–	-4.4588×10^{-4}
	253	0.40	0.4322	–	-4.2659×10^{-4}
		4.00	0.3641	0.09492	0.02305
		14.29	0.3532	0.08884	0.03207
		42.86	0.3241	–	-3.5284×10^{-4}
	223	0.40	0.4053	–	-8.5318×10^{-4}
		4.00	0.2316	0.1424	0.02305
		14.29	0.0572	0.2318	0.02164
		42.86	0.0862	–	-9.3033×10^{-5}

Fig. 9 Flowchart of predicting the mechanical parameters for HTPB propellant under different loading conditions

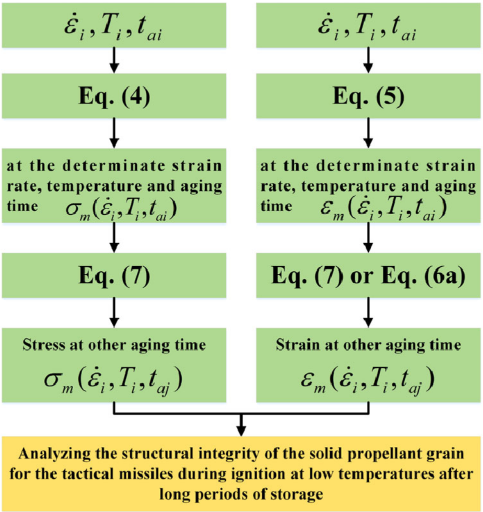
$\dot{\varepsilon}_i, T_i, t_{ai}$
$\dot{\varepsilon}_i, T_i, t_{ai}$
Eq. (4)
Eq. (5)
at the determinate strain rate, temperature and aging time $\sigma_m(\dot{\varepsilon}_i, T_i, t_{ai})$
at the determinate strain rate, temperature and aging time $\varepsilon_m(\dot{\varepsilon}_i, T_i, t_{ai})$
Eq. (7)
Eq. (7) or Eq. (6a)
Stress at other aging time $\sigma_m(\dot{\varepsilon}_i, T_i, t_{aj})$
Strain at other aging time $\varepsilon_m(\dot{\varepsilon}_i, T_i, t_{aj})$
Analyzing the structural integrity of the solid propellant grain for the tactical missiles during ignition at low temperatures after long periods of storage

knowledge of the properties for solid propellants under various loading conditions. Furthermore, a linear model and the improved exponential model were employed to describe the variation of the mechanical parameters with aging time in this investigation. Based on these models and the numerical expressions of the master curves, the tensile mechanical properties of HTPB propellant under different loading conditions (temperature, strain rate and aging time) can be predicted. Subsequently the related data can be provided for analyzing the structural integrity of the solid propellant grain for the tactical missiles during ignition at low temperatures after long periods of storage.

The obvious differences of the tensile behaviors for HTPB propellant before and after aging may seriously affect the structural integrity of the solid propellant grain for the tactical missiles during ignition at low temperatures after long periods of storage. In addition, strain at maximum tensile stress ε_m can be selected as a fail criterion for further analysis.

Acknowledgements The authors gratefully acknowledge the financial support of the National 973 Program in China (No. 61338) and the National Funds in China (Nos. 11772352, 61407200203 and 51328050101).

Publisher's Note Springer Nature remains neutral with regard to jurisdictional claims in published maps and institutional affiliations.

References

Andersen, P.C., Bruno, T.J.: Thermal decomposition kinetics of RP-1 rocket propellant. Ind. Eng. Chem. Res. **44**(6), 1670–1676 (2005)

Bohn, M.A., Volk, F.: Aging behavior of propellants investigated by heat generation, stabilizer consumption, and molar mass degradation. Propellants Explos. Pyrotech. **17**(4), 171–178 (1992)

Bunyan, P., Cunliffe, A.V., Davis, A., Kirby, F.A.: The degradation and stabilisation of solid rocket propellants. Polym. Degrad. Stab. **40**(2), 239–250 (1993)

Celina, M., Minier, L., Assink, R.: Development and application of tools to characterize the oxidative degradation of AP/HTPB/al propellants in a propellant reliability study. Thermochim. Acta **384**(1–2), 343–349 (2002)

Cerri, S., Bohn, M.A., Menke, K., Galfetti, L.: Ageing behaviour of HTPB based rocket propellant formulations. Central Eur. J. Energ. Mater. **6**(2), 149–165 (2009)

Cerri, S., Bohn, M.A., Menke, K., Menke, K., Galfetti, L.: Aging of HTPB/Al/AP rocket propellant formulations investigated by DMA measurements. Propellants Explos. Pyrotech. **38**(2), 190–198 (2013)

Chu, H.T., Chou, J.H.: Effect of cooling load on the safety factor of propellant grains. J. Propuls. Power **29**(1), 27–33 (2013)

de la Fuente, J.L.: An analysis of the thermal aging behaviour in high-performance energetic composites through the glass transition temperature. Polym. Degrad. Stab. **94**(4), 664–669 (2009)

de la Fuente, J.L., Rodrı´guez, O.: Dynamic mechanical study on the thermal aging of a hydroxyl-terminated polybutadiene-based energetic composite. J. Appl. Polym. Sci. **87**(14), 2397–2405 (2015)

Deng, B., Tang, G., Shen, Z.: Structural analysis of solid rocket motor grain with aging and damage effects. J. Spacecr. Rockets **50**(2), 331–339 (2015)

Edidin, A.A., Jewett, C.W., Kalinowski, A., Kwarteng, K., Kurtz, S.M.: Degradation of mechanical behavior in UHMWPE after natural and accelerated aging. Biomaterials **21**(14), 1451–1460 (2000)

Gligorijević, N., Živković, S., Subotić, S., Rodić, V., Gligorijević, I.: Effect of cumulative damage on rocket motor service life. J. Energ. Mater. **33**(4), 229–259 (2015)

Gligorijević, N.I., Rodić, V.Ž., Živković, S.Ž., Pavković, B.M., Nikolić, M.M., Kozomara, S.M., Subotić, S.D.: Mechanical characterization of composite solid rocket propellant based on hydroxy-terminated polybutadiene. Hem. Ind. **70**(5), 581–594 (2016)

Goncalves, R.F.B., Silva, R.P., Rocco, J.A.F.F., Iha, K.: Thermal decomposition kinetics of aged solid propellant based on ammonium perchlorate-AP/HTPB binder. AIAA 2008-4969 (2008)

Hocaoğlu, Ö., Pekel, F., Özkar, S.: Aging of HTPB/AP-based composite solid propellants, depending on the NCO/OH and Triol/Diol ratios. J. Appl. Polym. Sci. **79**(6), 959–964 (2001)

Husband, D.M.: Use of dynamic mechanical measurements to determine the aging behavior of solid propellant. Propellants Explos. Pyrotech. **17**(4), 196–201 (1992)

Jalocha, D., Constantinescu, A., Neviere, R.: Prestrained biaxial DMA investigation of viscoelastic nonlinearities in highly filled elastomers. Polym. Test. **42**, 37–44 (2015)

Jeremic, R.: Some aspects of time-temperature superposition principle applied for predicting mechanical properties of solid rocket propellants. Propellants Explos. Pyrotech. **24**(4), 221–223 (1999)

Jiang, S.P., Rui, X.T., Hong, J., Wang, G.P., Rong, B., Wang, Y.: Numerical simulation of impact breakage of gun propellant charge. Granul. Matter **13**, 611–622 (2011)

Judge, M.D.: An investigation of composite propellant accelerated ageing mechanisms and kinetics. Propellants Explos. Pyrotech. **28**(3), 114–119 (2003)

Kadiresh, P.N., Sridhar, B.T.N.: Experimental evaluation and simulation on aging characteristics of aluminised AP-HTPB composite solid propellant. Mater. Sci. Technol. **24**(4), 406–412 (2008)

Kadiresh, P.N., Sridhar, B.T.N.: Experimental study on ballistic behaviour of an aluminised AP/HTPB propellant during accelerated aging. J. Therm. Anal. Calorim. **100**(1), 331–335 (2010)

Kishore, K., Paiverneker, V.R., Prasad, G.: Effect of storage temperatures on the mechanical properties of the composite solid propellants. Combust. Sci. Technol. **19**, 107–118 (1979)

Kivity, M., Hartman, G., Achlama, A.M.: Aging of HTPB Propellant. AIAA 2005-3802 (2005)

Layton, L.H.: Chemical structural aging studies on HTPB propellant. ADA010731 (1975)

Lloyd, D.K.: Long-Range Service Life Analysis (LRSLA) estimating procedure. J. Spacecr. Rockets **14**(6), 351–357 (1977)

Reeling Brouwer, G., Keizers, H.: Aging in composite propellant grains. AIAA 2004-4058 (2004)

Reeling Brouwer, G., Weterings, F.P., Keizers, H.: Evaluation of ageing in composite propellant grains: Part 2. AIAA 2005-3803 (2005)

Rocco, J., Lima, J., Frutuoso, A., Iha, K., Ionashiro, M., Matos, J., Suárez-Iha, M.: Thermal degradation of a composite solid propellant examined by DSC. J. Therm. Anal. Calorim. **75**(2), 551–557 (2004)

Shekhar, H.: Studies on stress-strain curves of aged composite solid rocket propellants. Def. Sci. J. **62**(2), 90–94 (2012)

Trache, D., Khimeche, K.: Study on the influence of ageing on chemical and mechanical properties of N,N'-dimethyl-N,N'-diphenylcarbamide stabilized propellants. J. Therm. Anal. Calorim. **111**(1), 305–312 (2013)

Villar, L.D., Cicaglioni, T., Diniz, M.F., Takahashi, M.F.K., Rezende, L.C.: Thermal aging of HTPB/IPDI-based polyurethane as a function of NCO/OH ratio. Mater. Res. **14**(3), 372–375 (2011)

Wang, Z., Qiang, H., Wang, G., Huang, Q.: Tensile mechanical properties and constitutive model for HTPB propellant at low temperature and high strain rate. J. Appl. Polym. Sci. **132**(24) (2015a)

Wang, Z., Qiang, H., Wang, G.: Experimental investigation on high strain rate tensile behaviors of HTPB propellant at low temperatures. Propellants Explos. Pyrotech. **40**(6), 814–820 (2015b)

Wang, Z., Qiang, H., Wang, G., Wang, T.: A new test method to obtain biaxial tensile behaviors of solid propellant at high strain rates. Iran. Polym. J. **25**(6), 15–524 (2016a)

Wang, Z., Qiang, H., Wang, G., Zhu, Z.: Effects of low temperature and high strain rate on the tensile behaviors of high-performance energetic composite. In: MATEC Web of Conferences, vol. 67 (2016b)

Wang, Z., Qiang, H., Wang, T., Wang, G., Hou, X.: A thermovisco-hyperelastic constitutive model of HTPB propellant with damage at intermediate strain rates. Mech. Time-Depend. Mater. **22**(3), 291–314 (2018)
Yıldırım, H.C., Özüpek, Ş.: Structural assessment of a solid propellant rocket motor: effects of aging and damage. Aerosp. Sci. Technol. **15**(8), 635–641 (2011)
Zhao, Y.J., Zhang, W., Zhang, X.G., Zhu, H., Wang, C.H., Fang, L.J.: Aging property and storage life prediction of NEPE propellant. Theory Pract. Energ. Mater. **7**(1), 163–166 (2007)
Zou, X., Uesaka, T., Gurnagul, N.: Prediction of paper permanence by accelerated aging comparison of the predictions with natural aging results. Cellulose **3**(1), 269–279 (1996)
Zhou, D., Liu, X., Sui, X., Wei, Z., Wang, N.: Effect of pre-strain during ageing on the maximum elongation of composite solid propellants and its modelling. Polym. Test. **50**, 200–207 (2016)